3D printed multi-compartment capsular devices for two-pulse oral drug delivery

A. Maroni[1], A. Melocchi[1,2], F. Parietti[2], A. Foppoli[1], L. Zema[1], A. Gazzaniga[1]

[1]Università degli Studi di Milano, Dipartimento di Scienze Farmaceutiche, Sezione di Tecnologia e Legislazione Farmaceutiche "Maria Edvige Sangalli", 20133 Milan, Italy;

[2]Multiply Labs, 1760 Cesar Chavez Street Unit D, 94124 San Francisco, US-CA.

Corresponding author: Lucia Zema; Telephone: +39 02 503 24654; E - mail: lucia.zema@unimi.it

3D printed multi-compartment capsular devices for two-pulse oral drug delivery

Abstract

In the drug delivery area, versatile therapeutic systems intended to yield customized combinations of drugs, drug doses and release kinetics have drawn increasing attention, especially because of the advantages that personalized pharmaceutical treatments would offer. In this respect, a previously proposed capsular device able to control the release performance based on its design and compositions, which could extemporaneously be filled, was improved to include multiple separate compartments so that differing active ingredients or formulations may be conveyed. The compartments, which may differ in thickness and composition, resulted from assembly of two hollow halves through a joint also acting as a partition. The systems were manufactured by fused deposition modeling (FDM) 3D printing, which holds special potential for product personalization, and injection molding (IM) that would enable production on a larger scale. Through combination of compartments having wall thickness of 600 or 1200 μm, composed of promptly soluble, swellable/erodible or enteric soluble polymers, devices showing two-pulse release patterns, consistent with the nature of the starting materials, were obtained. Systems fabricated using the two techniques exhibited comparable performance, thus proving the prototyping ability of FDM versus IM.

Keywords

1. Introduction

Personalized medicine generally consists in tailoring medical treatments to meet the characteristics, needs and preferences of a single patient, thus involving purposely run diagnosis, therapy and follow-up [1,2]. With reference to the use of medicinal products, the goal would be to administer the right drug, at the correct strength and suitable time, in the most effective formulation, possibly matching the pharmacological therapy with the patient genotype and any other individual feature (*e.g.* allergies, intolerances, enzyme expression, anatomical/physiological characteristics). In support of therapy personalization, the Pharmacogenomics Knowledgebase was recently developed in order to collect information about the impact of human genetic variations on drug responses, and provide clinically relevant advices including dosing guidelines and drug labels [3-5]. Notably, about 10% of FDA-approved drug products, mainly in the oncology field, already report pharmacogenomic information (*i.e.* biomarkers) that help identify subgroups of patients that will most likely benefit from a specific treatment [6-9]. This approach may not only increase the safety and compliance associated with the pharmacological therapy but also reduce the healthcare system expenses by decreasing, for instance, the number of inpatient treatments due to adverse reactions and lack of adherence.

For personalization purposes, drug discovery and development within the pharmaceutical industry may require a shift from the current nature of linear processes to integrated ones with a series of feedback loops from clinical stages [10]. Thus, prompt and flexible adaptation of critical variables, such as the strength of the active ingredient, its release kinetics and administration mode, would ideally be possible at any step as a function of the diverse needs identified.

Consequently, manufacturing of individually-developed drug products might replace or complement large-scale fabrication of one-size-fits-all batches, thereby involving the use of suitable techniques that may even make real-time modification and point-of-care fabrication feasible. The

formulation of orphan drugs, galenical preparations and clinical trial samples could also benefit from such a new approach.

In the field of drug delivery, the design of advanced therapeutic systems able to provide versatile combinations of drugs, drug doses and/or release kinetics is desirable. Once-a-day fixed-dose combinations have mainly been proposed for prevention and treatment of cardiovascular disease (polypill) [11,12]. This approach is aimed at addressing the poor adherence issues related to the high daily number of prescribed therapeutics and dosing regimen complexity. Another drug combination tool was Dome matrix®, encompassing modular units obtained by tableting for either immediate or prolonged release. Upon combination, these units would enable administration of various drugs within a single dosage form, achievement of multiple kinetics and floating of the system [13,14]. More recently, functional containers in the form of capsules, able to convey differing formulations and control drug release according to the design and composition of the shell, were proposed [15-19]. The capsules were fabricated using injection molding (IM) that was proved suitable for the manufacturing of products with complex shape and challenging dimensions, having curvatures, cavities and details in the order of hundreds of microns [20]. As the shell components may be developed independent of the inner formulation and extemporaneously assembled, this delivery platform offers great flexibility, potential for customization and major expected benefits in terms of time-to-market as well as related costs. The possibility of a rapid prototyping thereof by fused deposition modeling (FDM) 3D printing, a technique involving extrusion of thermoplastic polymers and additive manufacturing based on digital models, was also demonstrated [21]. Interestingly, 3D printing has widely been exploited for the personalization of drug products [22-30]. By way of example, Khaled et al. exploited 3D printing by extrusion of liquid/semisolid materials for the fabrication of a polypill, *i.e.* an oral delivery system comprising various areas with different drug content and individual release performance [31,32].

Based on these premises, the aim of the present work was to devise and manufacture a versatile capsular delivery platform composed of separate compartments to be filled either with differing

active ingredients or with varied doses and/or formulations of one particular drug. Through combination of compartments having walls with differing compositions and thicknesses, in addition, such a device was intended to yield multiple release kinetics. In particular, promptly soluble, gastroresistant and swellable/erodible compartments were developed, which allowed immediate, enteric and pulsatile release to be achieved, respectively. By differently assembling these compartments, two pulse release patterns, characterized by one or more lag phases, could be obtained. The onset of release was expected to either be programmable in time or depend on the environmental pH. Time-dependent lag phases are of high current interest to meet chronotherapeutic needs related to widespread pathologies with circadian symptomatology, and as a strategy to pursue oral colon delivery [33,34]. Moreover, the availability of independent capsule compartments could especially be advantageous to simplify the dosing schedule in multitherapies involving active ingredients that may be mutually incompatible or interact in the gastrointestinal tract, thus positively impacting on overall patient compliance [35].

Both FDM and IM were used for the manufacturing of the capsular delivery platform. While the former would allow for personalization of the system, the latter would enable its production on a larger scale.

2. Materials and Methods

2.1. Materials

Polylactic acid (PLA) filament (L-PLA natural, ø 1.75 mm; MakerBot® Industries, US-NY); polyvinyl alcohol (PVA) filament (natural, ø 1.75 mm; German RepRap, D); hydroxypropyl methyl cellulose (HPMC; Affinisol™ 15cP, Dow, US-CA); hydroxypropyl methyl cellulose acetate succinate (HPMCAS; AQUOT-LG, Shin-Etsu, J); polyvinyl alcohol-polyethylene glycol graft copolymer (KIR; Kollicoat® IR, BASF, D); glycerol (GLY; Pharmagel, I); polyethylene glycol (PEG; PEG 400 and 8000, Clariant Masterbatches, I); triethyl citrate (TEC; Sigma Aldrich, D);

acetaminophen (AAP; Rhodia, I); blue and yellow dye-containing formulations (Kollicoat® IR Brilliant Blue and Kollicoat® IR yellow, BASF, D).

2.2. Methods

PLA and PVA filaments were used as received. After opening of the package, PVA filament was kept in oven at 40 °C. EC, HPMC, HPMCAS and KIR were kept in an oven at 40 °C for 24 h prior to use. Polymeric formulations, *i.e.* HPMC + 5% PEG 400, HPMCAS + 20% PEG 8000, KIR + 12% GLY, were prepared by mixing polymers with the selected plasticizer in a mortar. The amount of plasticizer was expressed as % by weight on the dry polymer.

2.2.1. Preparation of filaments

Filaments were prepared from polymeric formulations by hot melt extrusion (HME) using a twin-screw extruder (Haake™ MiniLab II, Thermo Scientific, US-WI) equipped with counter-rotating screws and a custom-made aluminum rod-shaped die (ø = 1.80 mm) as reported in [36]. Extruded rods were manually pulled and forced to pass through a caliper connected with the extruder and set at 1.80 mm. After production, filament diameter was verified every 5 cm in length, and portions having diameter out of the 1.75 ± 0.05 mm range were discarded.

2.2.2. Printing of capsular devices

FDM was performed by an adapted MakerBot Replicator 2 equipped with 0.4 mm and a 0.3 mm tips (MakerBot® Industries, US-NY; infill = 100%, layer height = 0.10 mm), using computer-aided design (CAD) files purposely developed as reported in the Results section. Each part of the capsular device was designed using Autodesk® Autocad® 2016 software version 14.0 (Autodesk, Inc., US-CA), saved in .stl format and imported to the 3D printer software (MakerWare Version 2.2.2.89, MakerBot® Industries, US-NY). Either the supplied PLA/PVA filaments or portions of at least 25 cm of the in-house prepared filaments were used. When changing the filament before a new printing process, the printer was

cleaned, and leveling of the build plate was performed following assembly of the heating chamber as reported in [36]. The printing temperature was set based on the thermal and mechanical behavior of each material.

2.2.3. Molding of capsular devices

Molded units were prepared using a bench-top micro-molding machine (BabyPlast 6/10P, Cronoplast S.L.; Rambaldi S.r.l., I) equipped with a mold for the manufacturing of capsule parts [16]. Polymeric formulations were loaded into the IM press through a hopper. By subsequently applying two injection pressures, the injection pressure P_1 (maintained for 2.5 sec) and the holding pressure P_2 (maintained for 1.5 sec), at a selected rate (r_1 and r_2, respectively) expressed as a percentage of the maximum one, the plasticating plunger (10 mm diameter) was moved forward (charge, C), thus injecting specific amounts of material into the mold cavity through a 1 mm nozzle. Differing temperatures (T_1-T_4) were set throughout the equipment; T_4 was the temperature set for the hot runner within the mold. The process conditions are reported in Table 1.

Table 1: IM operating conditions.

Polymeric formulation	T_1 (°C)	T_2 (°C)	T_3 (°C)	T_4 (°C)	C (mm)	P_1 (bar)	v_1 (%)	P_2 (bar)	v_2 (%)
KIR + 12% GLY	140	150	155	160	4.5	30	30	20	15
HPMC + 5% PEG 400	155	160	165	170	6	40	45	30	35
HPMCAS + 20% PEG 8000	150	155	160	170	5	50	40	35	30

2.2.4. Characterization of printed and molded capsular devices

Each part of the capsular devices was checked for weight (analytical balance BP211, Sartorius, D; n = 10) and thickness (MiniTest FH7200 equipped with FH4 probe, ø sphere = 1.5 mm, ElektroPhysik, D; n = 10). Digital photographs (Nikon D70, Nikon, J) of samples were also acquired. Resistance to deformation was measured by a TA-XT plus Texture Analyzer (ENCO, Spinea, I) equipped with a 5 kg load cell. A flat-ended probe of 10 mm in diameter was used,

In order to evaluate the release performance (n = 3), each compartment of the capsular devices was filled with 40 mg of AAP (cv ≤ 2). When swellable/erodible compartments were dealt with, the assembled capsules were inserted into sinkers and tested by a three-position USP38 disintegration apparatus (Sotax, CH) [15]. Each basket-rack assembly moved at a 31 cycles/min rate in a separate vessel filled with 800 mL of water at 37 ± 0.5 °C. When enteric soluble compartments were dealt with, the release performance was evaluated by USP38 apparatus 2 (Dissolution System 2100B, Distek, NJ-US) at 100 rpm, under the conditions of the "Dissolution Test for Delayed-Release Dosage Forms" (Method B, USP38). Fluid samples were withdrawn at fixed time points and assayed spectrophotometrically (λ = 248 nm). By linear interpolation of the release data immediately before and after the time point of interest, the following parameters were calculated: *i)* time to 10% release ($t_{10\%}$), which was used to define the lag phase of pulsatile-release and enteric soluble compartments; *ii)* time to 90% release ($t_{90\%}$), which was used to calculate the pulse time ($t_{90\%-10\%}$) of pulsatile-release compartments; *iii)* time to 80% dissolution ($t_{80\%}$), which was used to describe the performance of promptly-soluble compartments. With enteric soluble compartments, the duration of the lag phase before release in phosphate buffer was calculated as $t_{10\%}$ - 120 min.

PVA-based systems, in which each compartment was filled with approximately 40 mg of blue or yellow dye-containing formulations, were immersed in unstirred distilled water at 37 ± 0.5 °C, and digital photographs were taken at successive time points.

3. Results and discussion

3.1 Design of capsular devices

The capsular device under development was initially conceived in the form of a two-compartment shell composed of three parts: two hollow halves, each consisting in a cylindrical section with one rounded, closed end and one open end, and a middle part acting both as a joint and a partition. The joint would allow the hollow parts to be assembled into a closed device while dividing the internal cavity into two separate compartments (Figure 1). The hollow parts may differ in geometry and thickness, thus leading to compartments of same or different internal volume and/or wall thickness. Initially, the external shape of the hollow parts was maintained equal, while the wall thickness was set at 600 and 1200 µm.
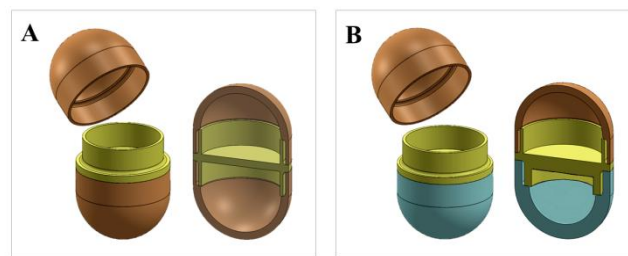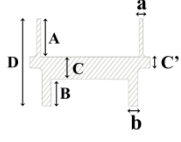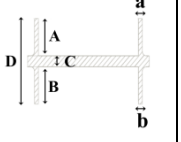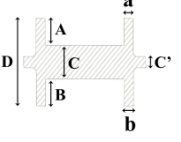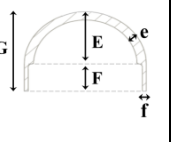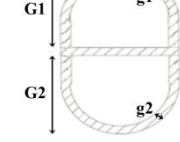

Figure 1: Isometric and cross-section views of two-compartment capsular devices either composed of halves with same (A) or different (B) thickness.

CAD files were thus created: two for the hollow parts relevant to compartments of 600 and 1200 µm nominal wall thickness, respectively, and three for joints that would allow halves having same (600 or 1200 µm) or different (600 and 1200 µm) nominal wall thickness to be coupled. Hollow parts and joints with halved thickness in the overlapping areas (closure) were designed, thereby leading to compartments of the final capsular device having constant wall thickness (Table 2). Moreover, the thicker-wall compartment had a smaller void inner volume, so that the assembled device could maintain the same height and width.

9

As a further development, the capsular device might include multiple inner compartments obtained by using more than one joint.

Table 2: Nominal dimensions of two-compartment capsular devices and relevant parts.

		Joint			Hollow half		Capsular device		
Height, mm	A	2.02	2.02	1.72					
	B	1.42							
	C (C')	1.20 (0.60)	0.60 (0.60)	1.20 (0.60)			(0.60)		
	D	4.64							
	E				4.18				
	F				2.02				
	G				6.20				
	G1								
	G2								
Thickness, mm	a	0.30	0.30	0.60					
	b	0.60							
	e				0.60	1.20			
	f				0.30	0.60			
	g1						0.60	1.20	0.60
	g2								1.20
Maximum width, mm		7.90							

3.2 Feasibility of FDM in fabrication of capsular devices

The feasibility of FDM in the manufacturing of the two-compartment capsular device was preliminarily investigated using a commercially available filament of PVA, which met the equipment requirements in terms of shape, diameter, diameter tolerances and mechanical properties. Two different tips were employed, namely the standard one having diameter of 0.4 mm and another characterized by a smaller diameter (0.3 mm), already shown useful to improve detail resolution [21]. Following the initial printing trials, the need for a stem, which may broaden the contact area between the build plate and the hollow item, thus preventing its collapse during fabrication, was
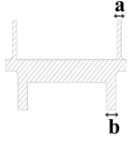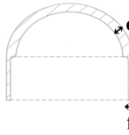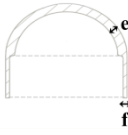
highlighted. Such a stem turned out necessary for the manufacturing not only of capsule halves, as expected based on previous experience, but also of joints. Therefore, CAD files had to be modified accordingly (Figure 2). When the stem was connected with the outer surface of the rounded, closed end of the hollow parts, it was possible to easily detach it at the end of the process (*i.e.* post-process). In the case of joints, however, removal of the stem was more critical. Improvements would thus be required in either the design or the printing procedure.

Figure 2: Isometric and cross-section views of a joint with cylindrical stem and photograph of the corresponding PVA printed item.

By adjusting process parameters, *e.g.* selecting the high resolution printing mode and a temperature of 210 °C, all components of capsular devices were successfully printed. Data relevant to printed PVA parts, to be assembled into a device having two compartments of 600 and 1200 μm nominal wall thickness, are reported in Table 3. Due to the presence of the stem, it was not possible to measure the thickness of the joint, indicated as "b" in the table.

Table 3: Weight and thickness of hollow and middle PVA parts of capsular devices having two compartments of 600 and 1200 µm nominal wall thickness, respectively, printed with different tips.

	Joint		Hollow half			
	a / b		e / f		e' / f'	
Tip diameter, mm	0.4	0.3	0.4	0.3	0.4	0.3
Weight, mg (cv)	106.40 (3.96)	110.06 (4.75)	103.63 (2.88)	103.63 (2.88)	145.24 (2.05)	159.19 (3.57)
Thickness, µm (cv) — a, 300*	467 (7)	377 (7)				
Thickness, µm (cv) — b, 600*	n.d.	n.d.				
Thickness, µm (cv) — e, 600*			627 (18)	643 (5)		
Thickness, µm (cv) — f, 300*			416 (15)	368 (5)		
Thickness, µm (cv) — e', 1200*					1134 (6)	1252 (3)
Thickness, µm (cv) — f', 600*					742 (9)	673 (7)

n.d. = not determined
*nominal thickness, µm

Weight data showed satisfactory reproducibility, which could be attributed to reliable characteristics of the starting filament. Differences with respect to nominal values were exhibited by thickness data, more pronounced and with higher variability in the case of capsule parts printed by the 0.4 mm tip. This could be due to difficulties in controlling the layer deposition process and tendency of the material to expand after deposition. The smallest nominal wall thickness that could be reached depended on the tip diameter. In effect, wall thicknesses of 300 µm could not even be obtained by the use of the 0.3 mm tip. The attainment of wall thicknesses greater than the nozzle diameter required that adjacent layers of fused material be more closely deposited or even partially superimposed, which is automatically implemented by the printer software and may not be fine-tuned on a case-by-case basis, for instance by compensating for the volumetric changes of the material. To overcome such resolution limitations, the digital model of the capsular device was provided with a gap between the overlapping portions of hollow and middle parts [21]. Gaps of

different size, in the 0.125 - 0.5 mm range, were introduced into the CAD files, by varying the external diameter of the middle part while keeping the internal diameter of the hollow halves constant. In this case, the gap size leading to perfectly matching and tightly closed devices was of 0.2 mm. Such a value needed to be reconsidered when using any other material.

The absence of breaches in the printed parts, the tightness of the locking mechanism and the opening behavior of each compartment of PVA capsular devices were then evaluated in aqueous medium. The changes undergone over time in unstirred water by a device including two compartments with wall thicknesses of 600 and 1200 µm, respectively, each containing a different dye, were first observed. In Figure 3, photographs of the system before testing and at successive time points during the test are reported.
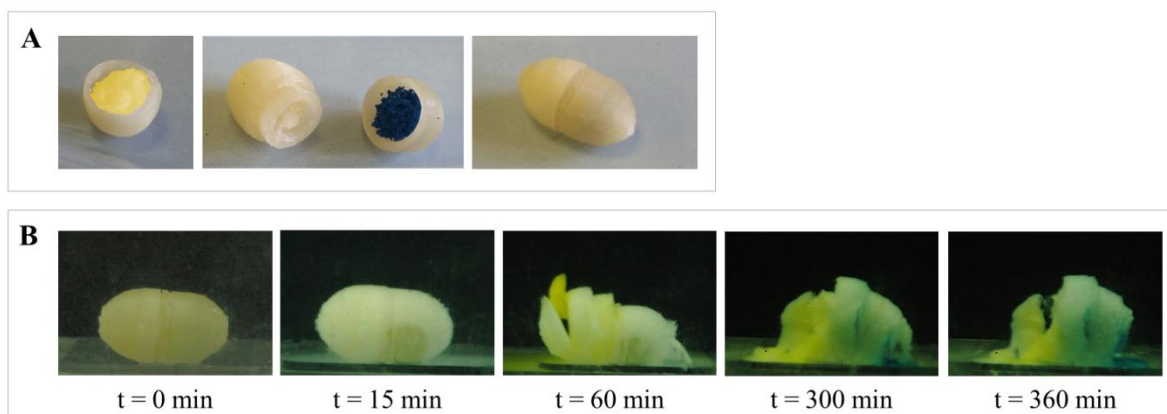

Figure 3: Capsular device including two compartments with wall thickness of 600 and 1200 µm filled with yellow and blue dyes, respectively, before (A) and during (B) immersion in unstirred water.

Dye leakage from the assembled device was noticed at about 60 min, thus proving the integrity of the printed capsule parts and the effectiveness of the locking system. Breaches first appeared in the thinner capsule half, particularly at the rounded area, as highlighted by leaching of the yellow dye. The higher wall thickness of the other compartment hindered penetration of the solvent inside the relevant cavity for longer. Leakage of the blue dye took place about 4 h later in the specular position of the device. Therefore, dependence of the release performance on the thickness of the

capsular device was demonstrated. In addition, PVA capsular devices showed a swellable/erodible behavior consistent with the nature of the starting material, with evidence of the formation of a gel layer and the dissolution of the polymer in water. Accordingly, the release profile of a capsular device filled with equal amounts of a drug tracer showed two pulses after about 15 and 50 min, due to successive opening of the 600 and 1200 μm thick compartments (Figure 4). The release of both fractions (*i.e.* pulses) of the tracer was prompt and quantitative.
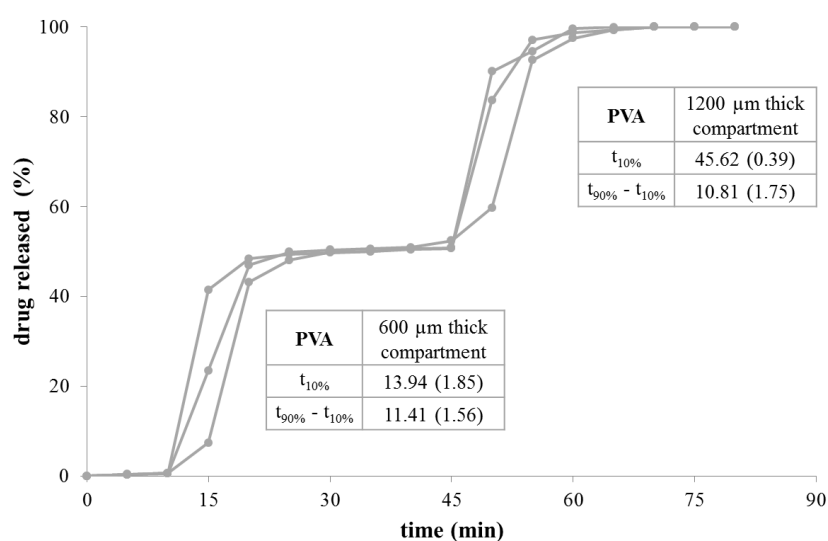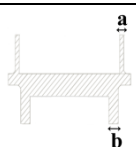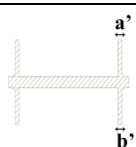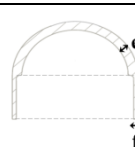

PVA	1200 μm thick compartment
$t_{10\%}$	45.62 (0.39)
$t_{90\%} - t_{10\%}$	10.81 (1.75)

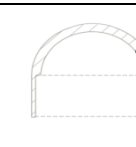| PVA	600 μm thick compartment
$t_{10\%}$	13.94 (1.85)
$t_{90\%} - t_{10\%}$	11.41 (1.56)

Figure 4: Release profiles of PVA capsular devices including two compartments with wall thickness of 600 and 1200 μm (release parameters and standard deviations, in brackets, are listed in boxes).

3.3 Manufacturing and evaluation of printed capsular devices

Once the feasibility of FDM in the manufacturing of the two-compartment capsular device was assessed, the performance of systems fabricated starting from pharmaceutical-grade polymers with different physico-chemical characteristics and recognized functionality in the field of drug delivery was investigated. Filaments based on a variety of these polymers were recently produced by HME, and their suitability for printing by FDM polymeric barriers having thickness values of hundreds of microns was demonstrated [36]. Thus, hollow capsule halves based on promptly soluble KIR,

swellable/erodible HPMC and enteric soluble HPMCAS were obtained and assembled. For the assembly of each capsular device, the joint was printed starting from the same material used for fabrication of the capsule half supposed to last longer as a barrier. As expected, the variability and deviation from the nominal value of the thickness of the printed parts turned out higher than when commercial PVA filament was employed (Table 4). This could reasonably be ascribed to the use of homemade filaments, which expectedly possess a lesser extent of finishing than commercially available ones, *e.g.* associated with higher variability in diameter and likelihood to undergo in-process morphology changes. However, by adjusting the gap betewen the hollow halves and the joint, it was possible to overcome the resolution limitations encountered and obtain tightly-closed assembled devices.

Table 4: Weight and thickness of hollow and middle parts of capsular devices based on different polymeric formulations.

			Joint		Hollow half	
			a / b	a' / b'	e / f	e' / f'
Weight, mg (cv)	KIR + 12% GLY				108.40 (7.71)	
	HPMC + 5% PEG 400		70.84 (6.55)	58.61 (4.93)	88.32 (5.64)	119.78 (5.68)
	HPMCAS + 20% PEG 8000		92.90 (10.95)	74.13 (8.90)	121.64 (11.75)	
Thickness, µm (cv)	KIR + 12% GLY	e, 600*			732 (11)	
		f, 300*			523 (14)	
	HPMC + 5% PEG 400	a, 300*	512 (11)			
		b, 600*	n.d.			
		a', 300*		530 (8)		
		b', 300*		n.d.		
		e, 600*			629 (18)	
		f, 300*			498 (12)	
		e', 1200*				1170 (17)
		f', 600*				643 (13)
	HPMCAS + 20% PEG 8000	a', 300*		478 (12)		
		b', 300*		n.d.		
		e, 600*			727 (13)	
		f, 300*			456 (15)	

*nominal thickness, µm

n.d. = not determined

Through combination of hollow parts of different wall thickness and composition, filled with a drug tracer, a variety of release profiles were obtained. In particular, two-pulse release patterns, expected on the basis of the nature of polymeric components, were observed. Examples are reported in Figure 5.

The capsular systems were confirmed to be tightly closed, as no drug tracer was detected prior to the release pulses. The performance of each compartment was demonstrated to depend on the relevant wall thickness and composition only, while being unaffected by those of the coupled compartment. In all cases, $t_{80\%}$ from hollow parts composed of KIR was of approximately 15 min, irrespective of the equipment employed, *i.e.* either dissolution apparatus or, when a swellable/erodible polymer compartment was dealt with, disintegration apparatus. Moreover, a lag phase prior to release of the tracer from HPMC compartments was observed, consistent with the hydration, swelling and dissolution/erosion of the polymeric wall barrier. The duration of such a lag phase proportionally increased with the wall thickness of the compartment ($t_{10\%}$ of about 55 min for 600 µm and 110 min for 1200 µm compartments). The subsequent release was prompt and complete within about 5 or 10 min, for 600 µm and 1200 µm thick units, respectively. Enteric soluble compartments showed the desired resistance in the acidic environment, and the shell started to dissolve when switching to pH 6.8 buffer medium. The release took place after a lag time due to the relatively high wall thickness of the compartment, as already observed [17]. The lack of a prompt and complete dissolution was also highlighted for enteric layers manufactured by coating [37].
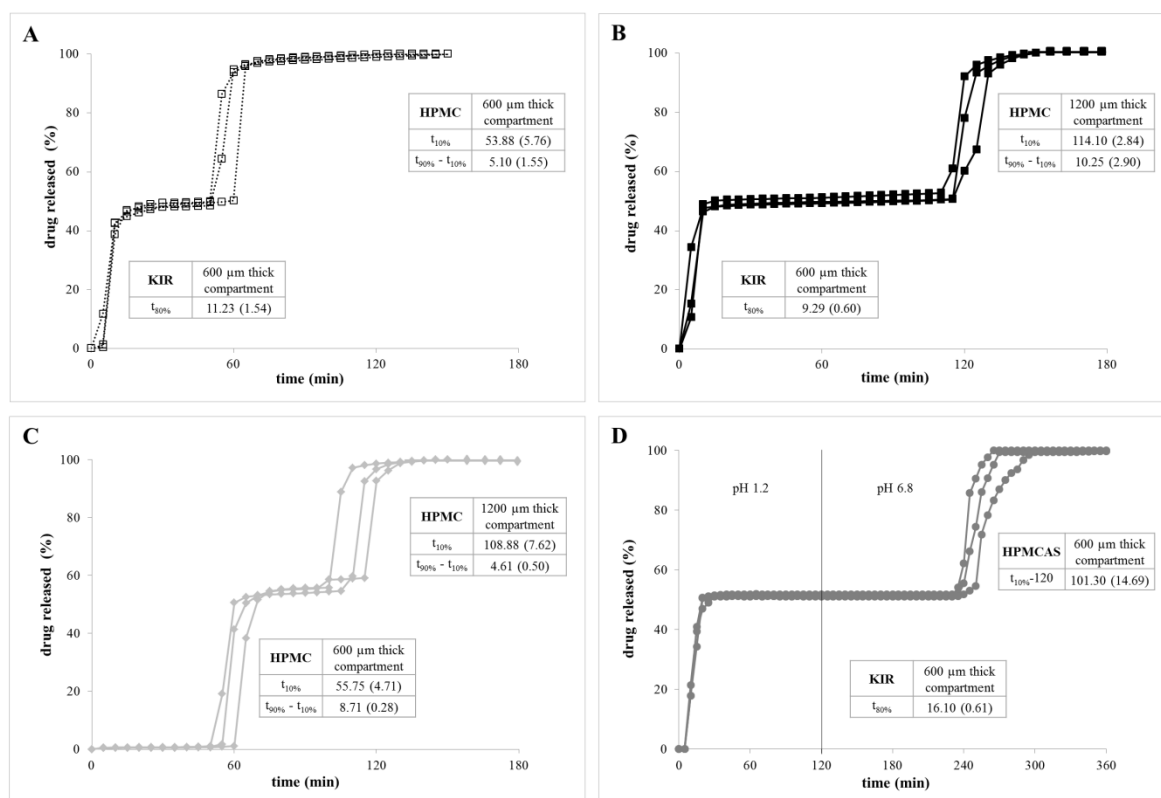
Figure 5: Release profiles of capsular devices including compartments having different wall thickness and composition: (A) 600 µm KIR and 600 µm HPMC compartments, (B) 600 µm KIR and 1200 µm HPMC compartments, (C) 600 µm HPMC and 1200 µm HPMC compartments and (D) 600 µm KIR and 600 µm HPMCAS compartments (release parameters and standard deviations, in brackets, are listed in boxes).

3.4 Manufacturing and evaluation of molded capsular devices

Based on the assessed versatility of release performance of the two-compartment capsular system, its components, *i.e.* hollow halves and joints, could be proposed for extemporaneous compounding of personalized medicines. These could be obtained by filling pre-formed shells having pre-determined release behavior with different drugs or drug formulations. In order to make larger-scale production of such shells feasible, a more cost-effective process than 3D printing should be identified. Previous results pointed out the real-time prototyping ability of FDM in the development of single-compartment capsule shells based on a swellable/erodible polymer manufactured by IM (*i.e.* Chronocap™ System) [21]. Therefore, the feasibility of IM in fabrication of two-compartment capsular devices was preliminarily evaluated. Molded hollow halves based on KIR, HPMC and

HPMCAS were fabricated using the mold previously employed for cap units [16]. At this stage of the work, the joint suitable for assembly of two caps of 600 μm in wall thickness was designed and produced by FDM. The printed joints could be used as prototypes for the development of relevant molds.

For comparison purposes, the polymeric formulations already employed for FDM were used as such in IM processing (Figure 6). By adjusting operating parameters, complete caps having acceptable physico-technological characteristics were obtained from all the materials under investigation. However, as the mold was specifically conceived for a hydroxypropyl cellulose-based formulation, the measured thickness of molded KIR, HPMC and HPMCAS parts turned out higher with respect to nominal values (differences < 10 %). Consequently, tightly closed devices could only be obtained by modulating the size of the gap between the cap, and the joint. More into detail, the external diameter of the cylincrical portion of the joint was progressively reduced in each CAD file until the resulting printed prototype could be matched with the cap, enabling thight closing. The need for purposely devised molds was indeed confirmed.
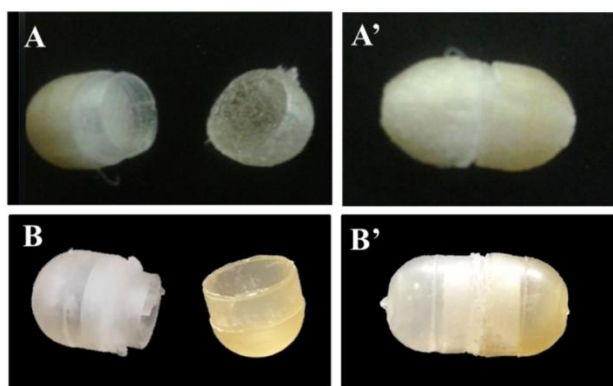

Figure 6: Photographs of partially assembled and assembled two-compartment capsular devices composed of 600 μm thick KIR and HPMC hollow parts fabricated by FDM (A, A') or IM (B, B').

The performance of two-compartment capsular devices based on promptly-soluble and swellable/erodible molded hollow parts was analogous to that achieved from printed units having

same design and composition. By way of example, the release profiles of capsules comprising two 600 μm thick molded compartments based on KIR and HPMC, respectively, are reported in Figure 7. A two-pulse release pattern was obtained: an immediate release profile of the drug tracer from the KIR compartment ($t_{80\%} \approx 15$ min) followed by a second pulse from the HPMC compartment after a lag phase ($t_{10\%} \approx 55$ min) analogous to that of the printed part. The time needed for a complete release from the swellable/erodible compartments (*i.e.* $t_{90\%}$ - $t_{10\%}$) also turned out comparable. Consistent results were obtained with differently-assembled two-compartment systems. The possibility to exploit FDM as a real-time prototyping tool for the development of molds dedicated to multi-compartment capsular devices was thereby demonstrated.
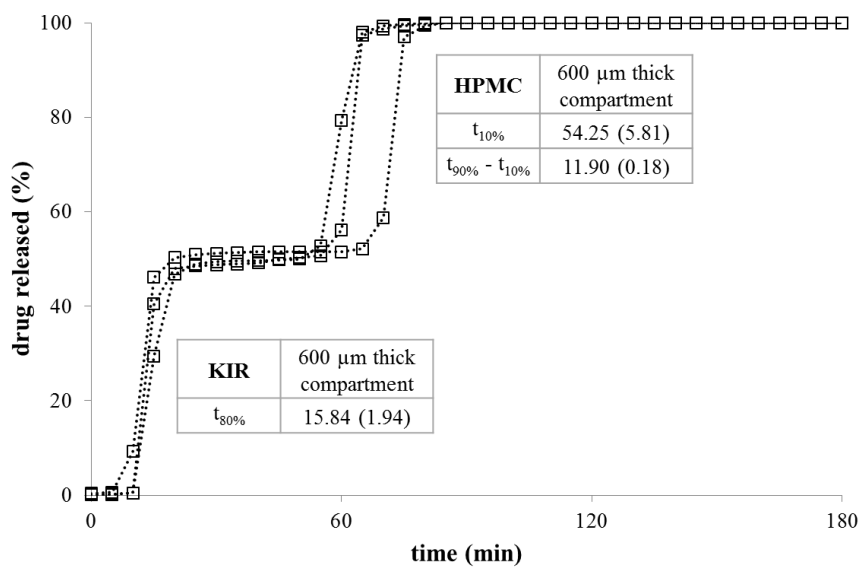

HPMC	600 μm thick compartment
$t_{10\%}$	54.25 (5.81)
$t_{90\%}$ - $t_{10\%}$	11.90 (0.18)

KIR	600 μm thick compartment
$t_{80\%}$	15.84 (1.94)

Figure 7: Release profiles of capsular devices including two 600 μm thick molded compartments based on KIR and HPMC (release parameters and standard deviations, in brackets, are listed in boxes).

Finally, in the prospect of an industrial-scale production of the two-compartment capsular device, it was deemed important to preliminarily assess the relevant mechanical resistance, which is expected to have a major impact on the outcome of filling, packaging and handling. A method previously proposed for the characterization of single-compartment molded capsules was adapted for

measurement of the mechanical resistance to deformation of hollow halves (Table 5) [15]. Data relevant to printed samples obtained from the commercially available PVA filament on the one hand, and having analogous composition as molded hollow parts on the other were also collected.

Table 5: Resistance to deformation of printed and molded hollow parts.

| | Resistance, N (cv) | | |
| | Printed hollow half | | Molded hollow half |
	600*	1200*	600*
PVA	7.87 (2.78)	40.64 (2.92)	
KIR + 12% GLY	8.75 (6.50)		25.00 (4.69)
HPMC + 5% PEG 400	6.83 (7.97)	16.83 (8.89)	35.46 (4.37)
HPMCAS + 20% PEG 8000	28.01 (12.71)		

*nominal thickness, µm

As expected, the resistance of samples to deformation turned out to depend on their thickness and on the material employed. Data were in relatively narrow range, thus pointing out reproducible mechanical behavior of both molded and printed parts. Hollow parts fabricated by FDM from homemade filaments showed slightly higher variability, as a consequence of their lower thickness consistency (Table 4). Resistance of molded hollow parts was in agreement with previous results relevant to hydroxypropyl cellulose capsular devices and greater than those obtained from bodies of gelatin capsules having closest size (19.08 N, cv 4.71) [16]. Such findings are of particular interest considering the industrial filling process, which the molded systems would be subjected to. When comparing printed and molded parts having analogous composition and thickness, the former turned out less resistant, reasonably because of the fabrication mode involved that is based on layer-by-layer addition of material. This feature could be improved by further promoting overlapping of contiguous layers and their mutual adhesion, *e.g.* by a post-process thermal treatment. Small batches of printed capsules, however, could extemporaneously be produced by coupling a purposely

developed powder-dosing system with the 3D printer to accomplish filling and shell fabrication in a single automated step.

4. Conclusions

Two-compartment capsular devices able to convey incompatible drugs or differing drug formulations were successfully manufactured using FDM as well as IM. Promptly soluble, swellable/erodible and enteric soluble polymers were employed as the starting thermoplastic materials. Through assembly of compartments having different wall thickness and/or composition, such a device was able to yield successive release pulses of a drug tracer. Versatile release profiles were achieved, and consistent results were obtained from systems fabricated by the two different hot-processing techniques under investigation. IM would be suitable for large-scale production of capsule shells having pre-determined release behavior, intended for subsequent filling in either pharmaceutical/nutraceutical industrial facilities or compounding pharmacies. The rapid prototyping ability of FDM was proved highly advantageous in the set-up of the design of the capsular system manufactured by IM. On the other hand, because FDM currently involves longer process times and is less cost-effective as compared with IM, it could only be exploited for production of small-sized batches. Moreover, it would enable real-time adjustment of the shell characteristics and, therefore, meet different patient needs, thus improving the extent of personalization of the drug therapy.

References

1. Jain K. K., 2009, Textbook of personalized medicine, Humana Press, second ed., Basel, pp. 1-3.

2. Zema L., Melocchi A., Maroni A., Gazzaniga A., 2017, 3D printing of medicinal products and the challenge of personalized medicine, J. Pharm. Sci., 106: 1697-1705.

3. Whirl-Carrillo M., McDonagh E. M., Hebert J. M., Gong L., Sangkuhl K., Thorn C. F., Altman R. B., Klein T. E., 2012, Pharmacogenomics knowledge for personalized medicine, Clin. Pharmacol. Ther., 92: 414-417.

4. Thorn C. F., Klein T. E., Altman R. B., 2013, PharmGKB: the pharmacogenomics knowledge base, Methods Mol. Biol., 1015: 311-320.

5. https://www.pharmgkb.org/, last access on August 3rd 2017.

6. Frueh F. W., Amur S., Mummaneni P., Epstein R. S., Aubert R. E., DeLuca T. M., Verbrugge R. R., Burckart G. J., Lesko L. J., 2008, Pharmacogenomic biomarker Information in drug labels approved by the United States Food and Drug Administration: prevalence of related drug use, Pharmacotherapy, 28: 992-998.

7. Kitzmiller J. P., Groen D. K., Phelps M. A., Sadee W., 2011, Pharmacogenomic testing: relevance in medical practice: why drugs work in some patients but not in others, Cleve Clin. J. Med., 78: 243-257.

8. Ventola C. L., 2011, Pharmacogenomics in clinical practice: reality and expectations, P. and T. 36: 412-416, 419-422, 450.

9. https://www.fda.gov/drugs/scienceresearch/researchareas/pharmacogenetics/ucm083378.htm, last access on August 3rd 2017.

10. Ginsburg G. S., McCarthy J. J., 2001, Personalized medicine: revolutionizing drug discovery and patient care, Trends Biotechnol., 19: 491-496.

11. Castellano J. M., Sanz G., Peñalvo J. L., Bansilal S., Fernández-Ortiz A., Alvarez L., Guzmán L., Linares J. C., García F., D'Aniello F., Arnáiz J. A., Varea S., Martínez F., Lorenzatti A., Imaz I., Sánchez-Gómez L. M., Roncaglioni M. C., Baviera M., Smith S. C., Taubert K.,

Pocock S., Brotons C., Farko M. E., Fuster V., 2014, A polypill strategy to improve adherence, J. Am. Coll. Cardiol., 64: 2071-2082.

12. Webster R., Rodgers A., 2016, Polypill treatments for cardiovascular diseases, Expert Opin. Drug Deliv., 13 1-6.

13. Losi E., Bettini R., Santi P., Sonvico F., Colombo G., Lofthus K., Colombo P., Peppas N. A., 2006, Assemblage of novel release modules for the development of adaptable drug delivery systems, J. Control. Release, 111: 212-218.

14. Strusi O. L., Sonvico F., Bettini R., Santi P., Colombo G., Barata P., Oliveira A., Santos D., Colombo P., 2008, Module assemblage technology for floating systems: in vitro flotation and in vivo gastro-retention, J. Control. Release, 129: 88-92.

15. Gazzaniga A., Cerea M., Cozzi A., Foppoli A., Maroni A., Zema L., 2011, A novel injection-molded capsular device for oral pulsatile delivery based on swellable/erodible polymers, AAPS PharmSciTech, 12: 295-303.

16. Zema L., Loreti G., Macchi E., Foppoli A., Maroni A., Gazzaniga A., 2013, Injection-molded capsular device for oral pulsatile release: development of a novel mold, J. Pharm. Sci., 102: 489-499.

17. Zema L., Loreti G., Melocchi A., Maroni A., Palugan L., Gazzaniga A., 2013, Gastroresistant capsular device prepared by injection molding, Int. J. Pharm., 440: 264-272.

18. Macchi E., Zema L., Maroni A., Gazzaniga A., Felton L. A., 2015, Enteric-coating of pulsatile-release HPC capsules prepared by injection molding, Eur. J. Pharm. Sci., 70: 1-11.

19. Macchi E., Zema L., Pandey P., Gazzaniga A., Felton L. A., 2016, Influence of temperature and relative humidity conditions on the pan coating of hydroxypropyl cellulose molded capsules, Eur. J. Pharm. Biopharm., 100: 47-57.

20. Zema L., Loreti G., Melocchi A., Maroni A., Gazzaniga A., 2012, Injection Molding and its application to drug delivery, J. Control. Release, 159: 324-331.

21. Melocchi A., Parietti F., Loreti G., Maroni A, Gazzaniga A., Zema L., 2015, 3D printing by fused deposition modeling (FDM) of a swellable/erodible capsular device for oral pulsatile release of drugs, J. Drug Deliv. Sci. Technol., 30 Part B: 360-367.

22. Alomari M., Mohamed F. H., Basit A. W., Gaisford S., 2015, Personalised dosing: printing a dose of one's own medicine, Int. J. Pharm., 494: 568-577.

23. Goyanes A., Det-Amornrat U., Wang J., Basit A. W., Gaisford S., 2016, 3D scanning and 3D printing as innovative technologies for fabricating personalized topical drug delivery systems, J. Control. Release, 234: 41-48.

24. Jonathan G., Karim A., 2016, 3D printing in pharmaceutics: a new tool for designing customized drug delivery systems, Int. J. Pharm., 499: 376-394.

25. Sandler N., Preis M., 2016, Printed drug-delivery systems for improved patient treatment. Trends Pharmacol. Sci., 37: 1070-1080.

26. Beck R. C. R., Chaves P. S., Goyanes A., Vukosavljevic B., Buanz A., Windbergs M., Basit A. W., Gaisford S., 2017, 3D printed tablets loaded with polymeric nanocapsules: an innovative approach to produce customized drug delivery systems, Int. J. Pharm., 528: 268-279.

27. Goyanes A., Fina F., Martorana A., Sedough D., Gaisford S., Basit A. W., 2017, Development of modified release 3D printed tablets (printlets) with pharmaceutical excipients using additive manufacturing, Int. J. Pharm. 527: 21-30.

28. Jamróz W., Kurek M., Łyszczarz E., Szafraniec J., Knapik-Kowalczuk J., Syrek K., Paluch M., Jachowicz R., 2017, 3D printed orodispersible films with aripiprazole, Int. J. Pharm., https://doi.org/10.1016/j.ijpharm.2017.05.052.

29. Norman J., Madurawe R. D., Moore C. M. V., Khan M. A., Khairuzzamana A., 2017, A new chapter in pharmaceutical manufacturing: 3D-printed drug products, Adv. Drug Deliv. Rev., 108: 39-50.

30. Okwuosa T. C., Pereira B. C., Arafat B., Cieszynska M., Isreb A., Alhnan M. A., 2017, Fabricating a shell-core delayed release tablet using dual FDM 3D printing for patient-centred therapy, Pharm. Res., 34: 427-437.

31. Khaled S. A., Burley J. C., Alexander M. R., Yang J., Roberts C. J., 2015, 3D printing of tablets containing multiple drugs with defined release profiles, Int. J. Pharm., 494: 643-650.

32. Khaled S. A., Burley J. C., Alexander M. R., Yang J., Roberts C. J., 2015, 3D printing of five-in-one dose combination polypill with defined immediate and sustained release profiles, J. Control. Release, 10: 308-314.

33. Palugan, L., Cerea M., Zema L., Gazzaniga A., Maroni A., 2015, Coated pellets for oral colon delivery. J. Drug Deliv. Sci. Technol., 25:1-15.

34. Maroni A., Zema L., Cerea M., Foppoli A., Palugan L., Gazzaniga A., 2016, Erodible drug delivery systems for time-controlled release into the gastrointestinal tract, J. Drug Deliv. Sci. Technol., 32: 229-235.

35. Maroni A., Zema L., Del Curto M.D., Loreti G., Gazzaniga A., 2010, Oral pulsatile delivery: rationale and chronopharmaceutical formulations, Int. J. Pharm., 398: 1-8.

36. Melocchi A., Parietti F., Maroni A., Foppoli A., Gazzaniga A., Zema L., 2016, Hot-melt extruded filaments based on pharma-grade polymers for 3D printing by fused deposition modeling, Int. J. Pharm., 509: 255-263.

37. Liu F., Lizio R., Meier C., Petereit H.-U., Blakey P., Basit A. W., 2009, A novel concept in enteric coating: a double-coating system providing rapid drug release in the proximal small intestine, J. Control. Release, 133: 119-124.

Figure captions

Figure 1: Isometric and cross-section views of two-compartment capsular devices either composed of halves with same (A) or different (B) thickness.

Figure 2: Isometric and cross-section views of a joint with cylindrical stem and photograph of the corresponding PVA printed item.

Figure 3: Capsular device including two compartments with wall thickness of 600 and 1200 μm filled with yellow and blue dyes, respectively, before (A) and during (B) immersion in unstirred water.

Figure 4: Release profiles of PVA capsular devices including two compartments with wall thickness of 600 and 1200 μm (release parameters and standard deviations, in brackets, are listed in boxes).

Figure 5: Release profiles of capsular devices including compartments having different wall thickness and composition: (A) 600 μm KIR and 600 μm HPMC compartments, (B) 600 μm KIR and 1200 μm HPMC compartments, (C) 600 μm HPMC and 1200 μm HPMC compartments and (D) 600 μm KIR and 600 μm HPMCAS compartments (release parameters and standard deviations, in brackets, are listed in boxes).

Figure 6: Photographs of partially assembled and assembled two-compartment capsular devices composed of 600 µm thick KIR and HPMC hollow parts fabricated by FDM (A, A') or IM (B, B').

Figure 7: Release profiles of capsular devices including two 600 µm thick molded compartments based on KIR and HPMC (release parameters and standard deviations, in brackets, are listed in boxes).

Table 1: IM operating conditions.

Polymeric formulation	T_1 (°C)	T_2 (°C)	T_3 (°C)	T_4 (°C)	C (mm)	P_1 (bar)	v_1 (%)	P_2 (bar)	v_2 (%)
KIR + 12% GLY	140	150	155	160	4.5	30	30	20	15
HPMC + 5% PEG 400	155	160	165	170	6	40	45	30	35
HPMCAS + 20% PEG 8000	150	155	160	170	5	50	40	35	30

Table 2: Nominal dimensions of two-compartment capsular devices and relevant parts.
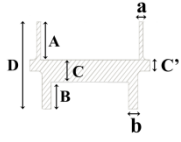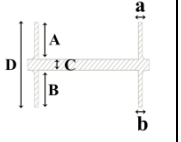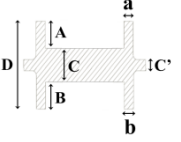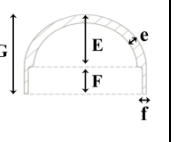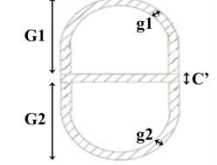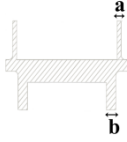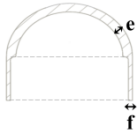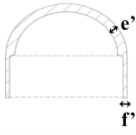
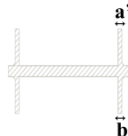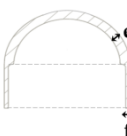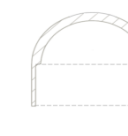|		Joint			Hollow half		Capsular device		
Height, mm	A	2.02	2.02	1.72					
	B	1.42							
	C (C')	1.20 (0.60)	0.60 (0.60)	1.20 (0.60)			(0.60)		
	D	4.64							
	E				4.18				
	F				2.02				
	G						6.20		
	G1								
	G2								
Thickness, mm	a	0.30	0.30	0.60					
	b	0.60							
	e				0.60	1.20			
	f				0.30	0.60			
	g1						0.60	1.20	0.60
	g2								1.20
Maximum width, mm		7.90							
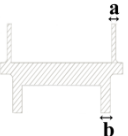
Table 3: Weight and thickness of hollow and middle PVA parts of capsular devices having two compartments of 600 and 1200 μm nominal wall thickness, respectively, printed with different tips.

		Joint		Hollow half			
Tip diameter, mm		*0.4*	*0.3*	*0.4*	*0.3*	*0.4*	*0.3*
Weight, mg (cv)		106.40 (3.96)	110.06 (4.75)	103.63 (2.88)	103.63 (2.88)	145.24 (2.05)	159.19 (3.57)
Thickness, μm (cv)	a, 300*	467 (7)	377 (7)				
	b, 600*	n.d.	n.d.				
	e, 600*			627 (18)	643 (5)		
	f, 300*			416 (15)	368 (5)		
	e', 1200*					1134 (6)	1252 (3)
	f', 600*					742 (9)	673 (7)

n.d. = not determined

*nominal thickness, μm

Table(s) 4

Table 4: Weight and thickness of hollow and middle parts of capsular devices based on different polymeric formulations.

			Joint		Hollow half	
			a / b	a' / b'	e / f	e' / f'
Weight, mg (cv)	KIR + 12% GLY				108.40 (7.71)	
	HPMC + 5% PEG 400		70.84 (6.55)	58.61 (4.93)	88.32 (5.64)	119.78 (5.68)
	HPMCAS + 20% PEG 8000		92.90 (10.95)	74.13 (8.90)	121.64 (11.75)	
Thickness, µm (cv)	KIR + 12% GLY	e, 600*			732 (11)	
		f, 300*			523 (14)	
	HPMC + 5% PEG 400	a, 300*	512 (11)			
		b, 600*	n.d.			
		a', 300*		530 (8)		
		b', 300*		n.d.		
		e, 600*			629 (18)	
		f, 300*			498 (12)	
		e', 1200*				1170 (17)
		f', 600*				643 (13)
	HPMCAS + 20% PEG 8000	a', 300*		478 (12)		
		b', 300*		n.d.		
		e, 600*			727 (13)	
		f, 300*			456 (15)	

*nominal thickness, µm

n.d. = not determined

Table 5: Resistance to deformation of printed and molded hollow parts.

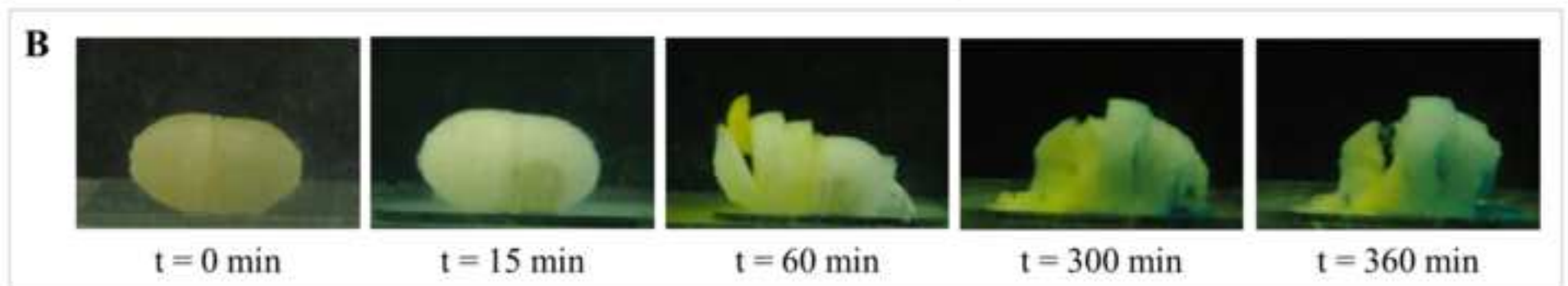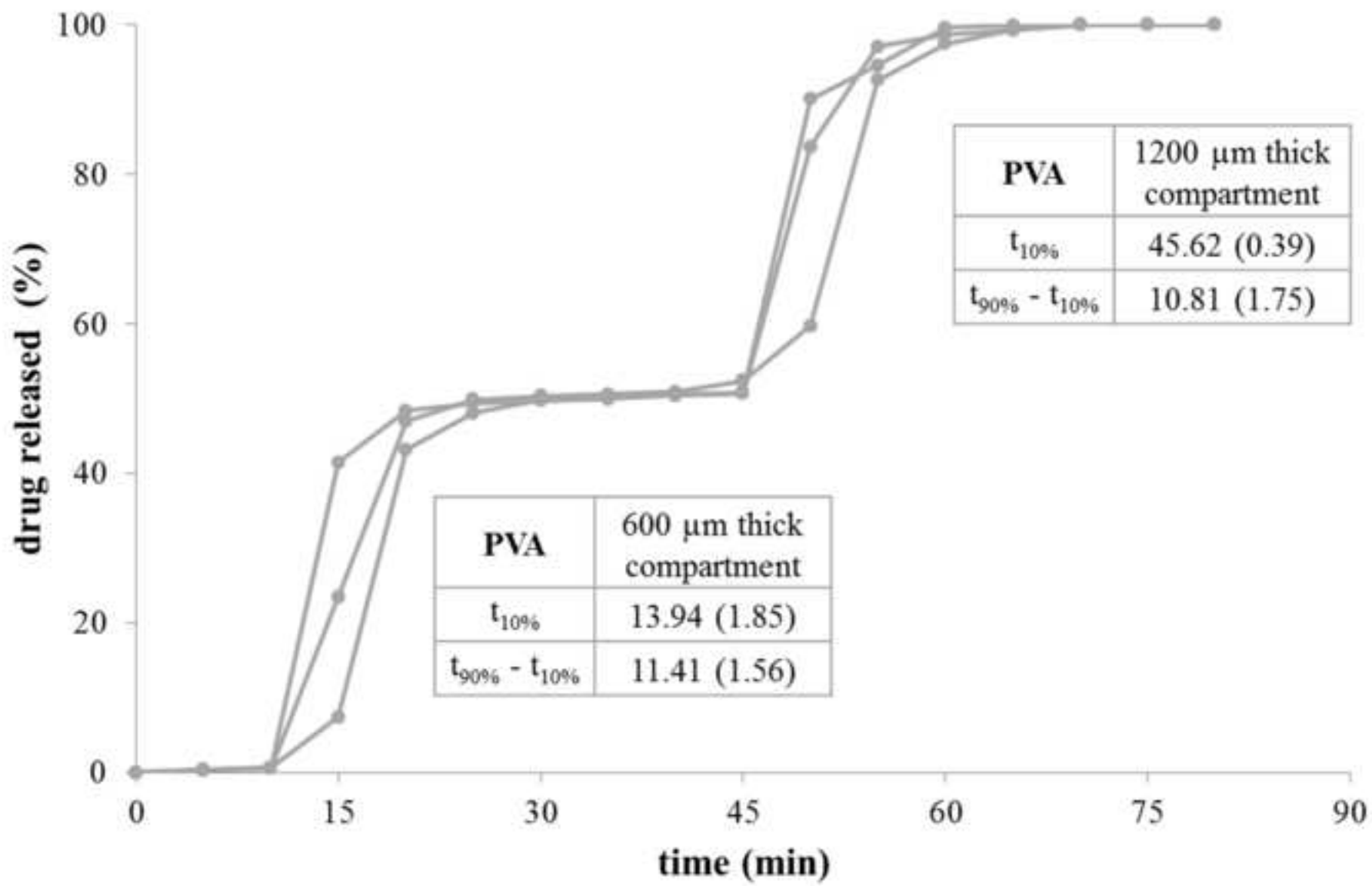|	Resistance, N (cv)		
	Printed hollow half		Molded hollow half
	600*	1200*	600*
PVA	7.87 (2.78)	40.64 (2.92)	
KIR + 12% GLY	8.75 (6.50)		25.00 (4.69)
HPMC + 5% PEG 400	6.83 (7.97)	16.83 (8.89)	35.46 (4.37)
HPMCAS + 20% PEG 8000	28.01 (12.71)		

*nominal thickness, μm

A

B

| t = 0 min | t = 15 min | t = 60 min | t = 300 min | t = 360 min |

PVA	1200 μm thick compartment
$t_{10\%}$	45.62 (0.39)
$t_{90\%} - t_{10\%}$	10.81 (1.75)

PVA	600 μm thick compartment
$t_{10\%}$	13.94 (1.85)
$t_{90\%} - t_{10\%}$	11.41 (1.56)

HPMC	600 μm thick compartment
$t_{10\%}$	54.25 (5.81)
$t_{90\%} - t_{10\%}$	11.90 (0.18)

KIR	600 μm thick compartment
$t_{80\%}$	15.84 (1.94)